Protein J (2015) 34:349–358
DOI 10.1007/s10930-015-9629-7

The Neuroprotective Role of Ferrostatin-1 Under Rotenone-Induced Oxidative Stress in Dopaminergic Neuroblastoma Cells

Parijat Kabiraj[1] · Carlos A. Valenzuela[2] · Jose E. Marin[1] · David A. Ramirez[1] · Lois Mendez[1] · Michael S. Hwang[1] · Armando Varela-Ramirez[2] · Karine Fenelon[2] · Mahesh Narayan[1] · Rachid Skouta[1]

Published online: 18 September 2015

Abstract Endoplasmic reticulum (ER) proteins including protein disulfide isomerase (PDI) are playing crucial roles in maintaining appropriate protein folding. Under nitrosative stress, an excess of nitric oxide (NO) radical species induced the S-nitrosylation of PDI cysteines which eliminate its isomerase and oxidoreductase capabilities. In addition, the S-nitrosylation-PDI complex is the cause of aggregation especially of the α-synuclein (α-syn) protein (accumulation of Lewy-body aggregates). We recently identified a potent antioxidant small molecule, Ferrostatin-1 (Fer-1), that was able to inhibit a non-apoptotic cell death named ferroptosis. Ferroptosis cell death involved the generation of oxidative stress particularly lipid peroxide. In this work, we reported the neuroprotective role of ferrostatin-1 under rotenone-induced oxidative stress in dopaminergic neuroblastoma cells (SH-SY5Y). We first synthesized the Fer-1 and confirmed that it is not toxic toward the SH-SY5Y cells at concentrations up to 12.5 μM. Second, we showed that Fer-1 compound quenched the commercially available stable radical, the 2,2-diphenyl-1-picrylhydrazyl (DPPH), in non-cellular assay at 82 %. Third, Fer-1 inhibited the ROS/RNS generated under rotenone insult in SH-SY5Y cells. Fourth, we revealed the effective role of Fer-1 in ER stress mediated activation of apoptotic pathway. Finally, we reported that Fer-1 mitigated rotenone-induced α-syn aggregation.

Keywords Ferrostatin-1 · Oxidative stress · Rotenone · α-synuclein · Apoptosis · Protein disulfide isomerase (PDI) · Endoplasmic reticulum stress · Inducible nitric oxide synthase · SH-SY5Y dopaminergic neuroblastoma cells

Abbreviations

ER	Endoplasmic reticulum
PDI	Protein disulfide isomerase
α-syn	α-synuclein
DPPH	2,2-diphenyl-1-picrylhydrazyl
Fer-1	Ferrostatin-1
PD	Parkinson's disease
ROS	Reactive oxygen species
RNS	Reactive nitrogen species
RT	Rotenone
Hsp70	70 kilodalton heat shok protein

1 Introduction

Oxidative and nitrosative stress caused by radical species such as reactive oxygen species (ROS) and nitrogen species (RNS) including nitric oxide (NOx) [1], are implicated in a wide array of human diseases [2], including neurological disorders [3]. Among the most common neurological disorders in the United States and the world are Alzheimer's (AD), Parkinson's (PD) and Lewy body dementia diseases

Electronic supplementary material The online version of this article (doi:10.1007/s10930-015-9629-7) contains supplementary material, which is available to authorized users.

✉ Mahesh Narayan
mnarayan@utep.edu

✉ Rachid Skouta
rskouta@utep.edu

[1] Department of Chemistry, The University of Texas at El Paso, 500 W. University Ave., El Paso, TX 79968, USA

[2] Department of Biological Sciences, Border Biomedical Research Center, The University of Texas at El Paso, 500 W. University Ave., El Paso, TX 79968, USA

[4]. While the exact mechanisms of each disease is still under debate, some researchers believe that the cause of the diseases is the increased of misfolded proteins in the cytosol of human neuronal cells caused by the development of the Lewy bodies [5]. Others believe that these misfolded proteins are unlikely to be the cause of the diseases but may be affecting the mitochondria dysfunction that is associated with the diseases [6]. For example, under physiological conditions, the mitochondrial complex III is the principal site of the generation of radical species in excess (e.g., ROS, RNS) which progress to activation of the apoptotic intrinsic pathway [7]. Rotenone is a one of the known ROS generator that triggered the production of NOx in mitochondria via apoptosis [8]. The mitochondria dysfunction is initiated by an increase of reactive species that triggered an imbalance of free radicals and antioxidant defenses, protein synthesis, folding, modification, trafficking and degradation that affect the endoplasmic reticulum (ER) in eukaryotic cells [9]. ER proteins including protein disulfide isomerase (PDI) are playing crucial roles in maintaining appropriate protein folding [10]. Under nitrosative stress, an excess of nitric oxide (NO) radical species, induced a chemical reaction between the PDI and nitric oxide. This chemical reaction generated a covalently bound formation of the S-nitrosyl of PDI cysteines (Fig. 1a) [11, 12] which eliminates its ability to (i) contribute in the oxidoreductase mechanism via the thiol-disulfide exchange reactions and (ii) diminish the neuronal cell death triggered by protein misfolding. Protecting the PDI from this chemical reaction (S-nitrosylation-PDI complex formation) make PDI an attractive therapeutic target in preventing neurodegeneration [13]. Previous work showed that the use of natural and non-natural compounds such as curcumin, and masoprocol [14], diphenyl difluoroketone (EF-24) [15] and ellagic acid [16] prevented the formation of S-nitrosylation of PDI and avoided protein aggregation. These compounds are known for their antioxidant and NOx radical trapping properties. Recently, an in silico and high-throughput screening [17] allow the identification of Fer-1, (Fig. 1b), as inhibitor of lipid ROS production. We then showed that Fer-1 prevents glutamate-induced neurotoxicity in a model of organotypic hippocampal slice culture (OHSC) [17]. Fer-1 was protective in cellular models such as Huntington's disease [18]. We also created a Fer-1 analog with improved stability that decreased the cell death in an in vivo model of renal tubule necrosis [19]. In this work, we will pursue the hypothesis that it is possible to investigate the neuroprotective effect of Fer-1 (Fig. 1b) under rotenone-induced oxidative stress in dopaminergic neuroblastoma cells (SH-SY5Y). We synthesized the Fer-1 in the laboratory based on our recently reported work [18]. Our results reveal that Fer-1 attenuated the apoptotic stimuli provoked by rotenone.

2 Materials and Methods

2.1 1,1-diphenyl-1-picrylhydrazyl (DPPH) Assay

The stable radical 2,2-diphenyl-1-picrylhydrazyl (DPPH) [20] was dissolved in methanol to a final working concentration of use 50 μM. This was prepared as follows. First, a 100 × stock concentration (5 mM) was prepared by dissolving 3.9 mg DPPH in 2 mL methanol. Then, for 25 mL of 50 μM final working solution, 250 μL of the 5 mM solution was added to 24.75 mL of methanol. 1 mL of DPPH solution was added to a small volume (<5 μL) each test compound dissolved in DMSO. The final concentration of each test compound was 50 μM. Then, 10 μL of each of the compound stock solution was added to one of the 96-Well Plate containing 190 μL of methanol, for a final volume of 200 μL and a final concentration of 100 μM. From there, 2 fold dilutions were made to obtain final concentrations of 100, 50, 25, 12.5 and 6.25 μM. Samples were then aliquoted to white 96-well solid-bottom dishes (Corning) and absorbance at 517 nm was recorded using a TECAN M200 plate reader. All values were normalized to background (methanol only). The experiment was repeated three times and the data was averaged.

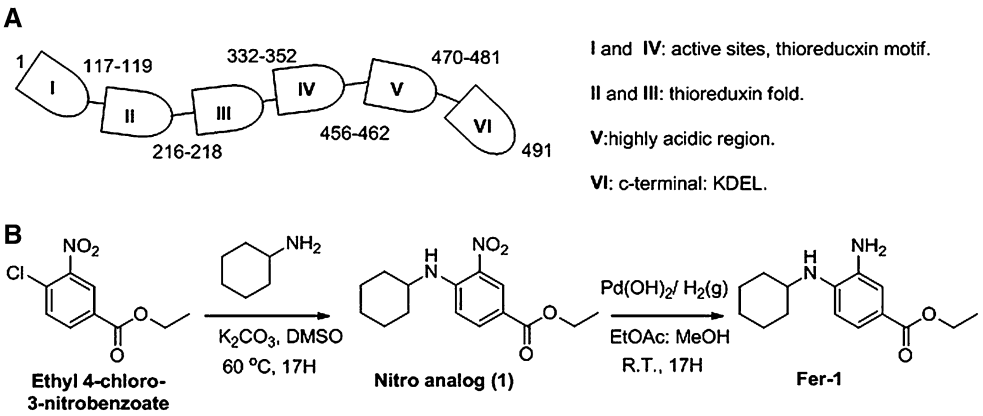

Fig. 1 **a** Schematic of PDI. **b** Synthesis of Fer-1(**2**). Conditions. step 1: cyclohexylamine, K_2CO_3, DMSO, 60 °C, 17H; step 2: $Pd(OH)_2$, H_2, EtOAc, MeOH, R.T., 17H

The radical scavenging effect will be calculated using the formula below:

$$\text{DPPH scavenging} = [(A_0 - A_1)/A_0] \times 100,$$

where A_0 is the absorbance of the methanol control and A_1 is the absorbance of Fer-1.

2.2 Cell Culture

The SH-SY5Y cells stably transfected with α-synuclein (α-syn) were cultivated at 37 °C in 5 % CO_2 with DMEM/F-12 media supplemented with 10 % (v/v) fetal bovine serum and 1 % (v/v) antibiotic (10,000 I.U/mL and 10,000 µg/mL). The Fer-1 and rotenone were dissolved in dimethyl sulfoxide (DMSO). The following treatments were applied to the SH-SY5Y cells: DMSO (0.02 %), rotenone, Fer-1.

2.3 Morphological Analysis of SH-S5Y Cells Exposed to Rotenone

SH-S5Y cells were seeded in 24-well plates as described above. After overnight incubation, the cells were exposed for 24 h to 500 nM of rotenone and also a mixture of 500 nM of rotenone plus 1 µM of Fer-1, under standard growth conditions. Independently, also cells treated with Fer-1 alone, solvent control (0.2 % v/v DMSO), H_2O_2 (50 µM) and untreated were included in this series of experiments. Brightfield photomicrographs were captured using an inverted microscope equipped with 10× objective in a live-cell modality and assisted with Micron USB2.0 software (Westover Scientific, ThermoFisher Scientific, Grand Island, NY). Image processing and exporting to TIFF format was achieved via Adobe Photoshop CS6 software (Adobe, San Jose, CA).

2.4 ROS and RNS Assays

Cells (2.0×10^4) were seeded (96-well plate) and incubated for 24 h before any treatment. DMEM/F-12 complete media without phenol red was used for these experiments. Cells were independently incubated with 50 µL of 20 µM 2′,7′-dichlorodihydro-fluoresceindiacetate (DCFH-DA) or 50 µL of a 7 µM 4-amino-5-methylamino-2′,7′-difluoro-fluoresceindiacetate (DAF-FM), utilized as ROS or RNS reporters, respectively. DCFH-DA and DAF-FM are membrane-permeable compounds that remain trapped into the cell after being processed by cellular esterase. Cells were washed with 1X PBS and treated with compounds. After treatment, cells were analyzed using a microplate reader Fluorometer (Lab systems Fluoroskan Ascent) at an excitation wavelength of 485 nm and emission of 527 nm for DCFH-DA and at an excitation wavelength of 485 nm and emission of 518 nm for DAF-FM. Each result is the compilation of two experimental repetitions.

2.5 Protein Isolation

The cells treated for 24 h with Fer-1 followed for 20 h with rotenone, were washed three times with phosphate-buffered saline (PBS) and pelleted by centrifugation. The supernatant was removed and 80 µL of lysis buffer was added to the cells and then stored overnight at −20 °C. Subsequently, the cells were centrifuged at 10,000 RPM for 12 min and both the pellet and supernatant were stored for future use.

2.6 SDS PAGE and Western Blot

Protein extracts were separated by using 12 % SDS gels. After electrophoresis, proteins were transferred onto a PVDF membrane and blocked with 5 % skim milk in TBST for 30 min. A series of different antibodies were then applied, the primary antibodies were applied for overnight treatment at 4 °C and the secondary antibody treatment was applied for about 1–2 h at room temperature. Protein bands were visualized by incubating the membranes with enhanced chemiluminescence reagent and exposed to x-ray films as previously described [21–22].

2.7 Confocal Microscopy

Cells were seeded over coverslip in the 6-well plates and grown to 80–90 % confluence. After 24 h of treatment with different compounds the cells were washed gently three times with PBS and then fixed by applying 100 % methanol for 2–3 min at −20 °C. The cells were then washed with PBS three times and blocked by incubating for 2 h at room temperature with 5 % (v/v) of NGS in PBS. Then, cells were incubated overnight at 4 °C with a solution containing anti α-syn rabbit primary antibody prepared at a 1:500 dilution in 5 % (v/v) NGS in PBS. Next, cells were washed three times with PBS and incubated for 2 h at room temperature in the dark with the Texas Red-conjugated goat anti-rabbit diluted at 1:1000 in 5 % (v/v) NGS in PBS, washed, DAPI counter-stained and mounted onto slides for visualization purposes. High-resolution images were acquired as previously described [21].

2.8 Immuno-blot, Immuno-fluorescence and Inclusion Body Quantification

The Image J software was used to quantify protein expression and fluorescence intensity.

Each image was converted into RGB file (8 bit). Random fields were chosen at the same magnification (63×) in

order to quantify the fluorescence of proteins. A region of interest (ROI) with an area of 400 pixels (20 × 20) was consistently chosen within subcellular location and the average of fluorescence intensity signal per pixel within the ROI was measured. Over 200 cells were analyzed for each condition. The values obtained were averaged and plotted using excel-bar graph. The results were obtained from three independent experiments.

2.9 Statistical Calculation

The results were represented as the mean and standard deviation of three replicates. Unpaired student's *t* test was calculated for significance testing with a P value <0.05 considered significant.

3 Results

3.1 Synthesis, DPPH Assay and Cytotoxicity of the Nitro-analog 1 and Fer-1

Figure 1b shows the synthesis of the Fer-1 compound. We synthesized the Fer-1 in the laboratory based on our recently reported work in two chemical transformations [17, 18]. Briefly, a nucleophilic aromatic substitution reaction (SNAr) between the commercially available ethyl 4-chloro-3-nitrobenzoate and cyclohexylamine in the presence of potassium carbonate and DMSO provided the nitro-analog compound **1** which was reduced under catalytic hydrogenolysis conditions ($Pd(OH_2)/H_2$) in a mixture of ethylacetate and methanol) to provide the desired ethyl 3-amino-4-(cyclohexylamino)benzoate (Fer-1) (Fig. 1b). The (Fer-1) was purified using column chromatography on silica gel and characterized using nuclear magnetic resonance (NMR) and liquid chromatography coupled mass spectrometry (LC/MS). The Fer-1 was fully characterized using Nuclear Magnetic Resonance 1H NMR, 13 NMR and LC/MC (see Fig. S1–3). We used our established DPPH stable free radical assay [17, 18], a sample colorimetric assay, to assess the ability of our compounds (**1** and **2**) to quench radical species. We previously reported that Fer-1 compound quenched the DPPH stable free radical at 82 % compared to DMSO control [17, 18]. Figure 3a shows the cytotoxicity study of the nitro-analog **1** and Fer-1 compounds. We determined the cytotoxicity of these compounds against dopaminergic neuroblastoma SH-SY5Y cells at various concentrations (3.13, 6.25 and 12.5 μM). We assessed the cell death of each concentration of each compounds. We observed only 3 % of cell death occurred at 12.5 μM of Fer-1. On the other hand no cell death was observed when treating the SH-SY5Y cells with 3.13 and 6.25 μM respectively. However the nitro analog **1** showed cytotoxicity at 12.5 μM with 20 % cell death (Fig. 3a).

3.2 Fer-1 Mitigated Rotenone-induced Cell Morphological Changes

To study the cellular morphological changes induced by rotenone and the potential protective effect of Fer-1 rescuing the stress response provoked by rotenone, microscopy approach was used to visualize changes on SH-S5Y cells morphology aspect. Rotenone-treated cells (500 nM) exhibited noticeable distortions of typical morphology, from spread to round, smaller in size, shrunken, detachment from the monolayer in cultures and forming cell aggregates (Fig. 2a; black arrows); these changes were also noted in H_2O_2-treated cells used as positive control for cytotoxicity (Fig. 2f; black arrows). Cells treated with a mixture of rotenone (500 nM) plus Fer-1 (1 μM) appeared with typical unstressed morphology (Fig. 2b), as compared with just Fer-1-treated cells, solvent (DMSO) treated and untreated cells, showing healthy and undamaged appearance (Fig. 2c–e), respectively. Findings suggest that Fer-1 was able to rescue the rotenone-induced neurotoxic cellular morphological alterations.

3.3 ROS and RNS Assay

Figure 3b, c shows the ROS and RNS assay respectively. We used the SH-SY5Y cells that were treated with 1 μM rotenone in the presence of 2′,7′-dichlorodihydro-fluoresceindiacetate (DCFH-DA) or a 7 μM 4-amino-5-methylamino-2′,7′-difluoro-fluoresceindiacetate (DAF-FM), utilized as ROS or RNS reporters, respectively. We observed that rotenone treatment exhibited a 1.68X fold increased in intracellular levels of RNS as compared to the negative control (Fig. 3b, c). Cells pretreated with 0.4 μM Fer-1 compound prior to a 1 μM RT exposure displayed significantly reduce intracellular RNS below basal levels (0.97X; $P < 0.0001$). However, negative control and 0.4 μM Fer-1 compound pretreatment + 1 μM RT treated cells shows similar RNS values, indicative of Fer-1 protection effect ($P = 0.360546$) as expected. Additionally, increased intracellular ROS levels (2.24X fold change) induced by a 1 μM RT treatment were also significantly lowered below basal levels (0.86X fold change; $P < 0.0001$) by a 0.4 μM Fer-1 pretreatment. Furthermore, the 1 μM RT + 0.4 μM Fer-1 condition shows a statistically significant decrease ($P = 0.0080$) in intracellular ROS levels when compared to the negative control.

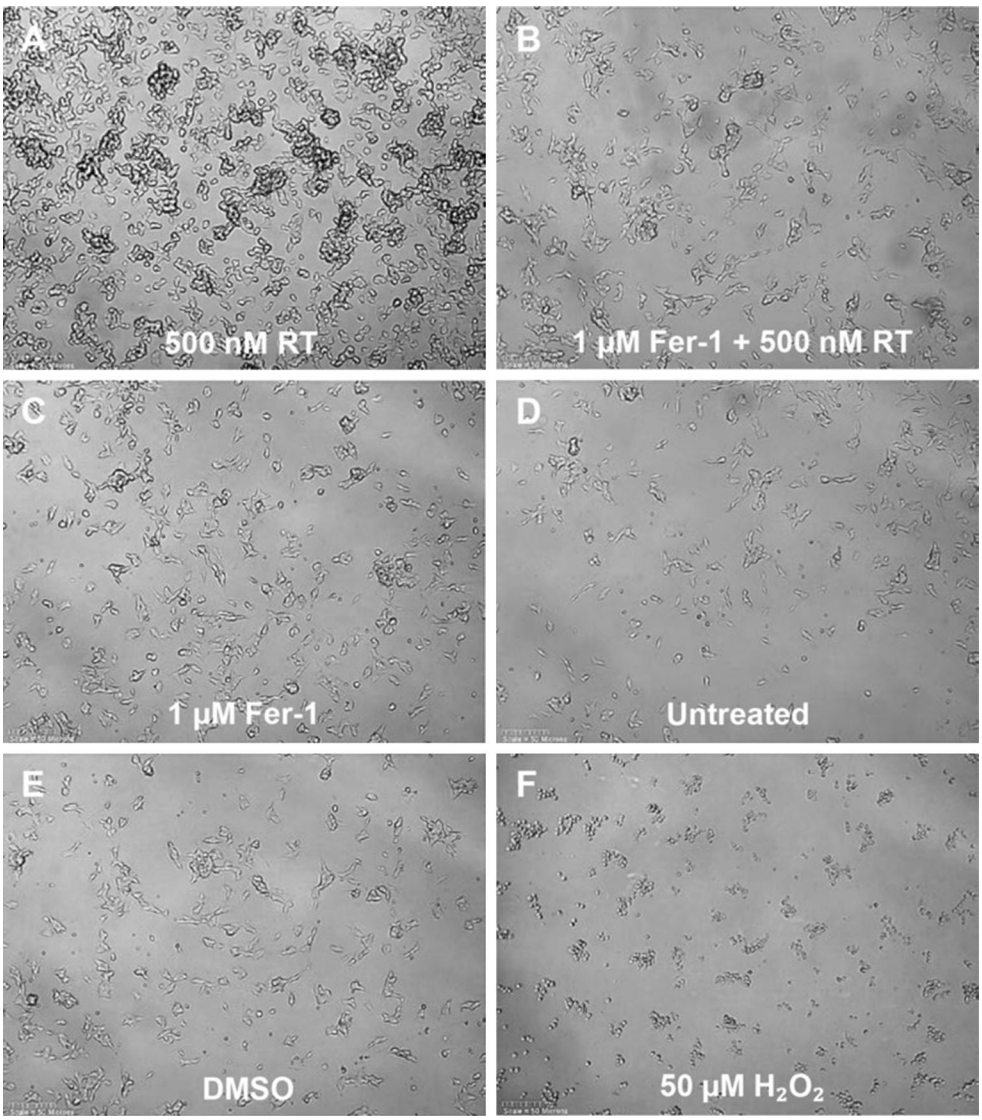

Fig. 2 Fer-1 rescued rotenone-induced morphological changes on SH-S5Y cells, after 24 h of treatment. Depicted are representative microscopic photomicrographs of cells treated with 500 nM of rotenone alone (**a**); 500 nM of rotenone plus 1 μM Fer-1 mixture (**b**); 1 μM Fer-1 alone (**c**); untreated (**d**); 0.2 % v/v DMSO (**e**); and 50 μM H_2O_2 as positive control of cytotoxicity (**f**). *Black arrows* are indicating loss of typical morphological of attached cells to spherical cell aggregates. *Scale bar* of 50 μm included in the *bottom right panel* (**f**) also applies to the rest of the panels

3.4 Role of Fer-1 Attenuating Rotenone-induced PARP-1 Cleavage

Figure 4 shows the anti-apoptotic ability of Fer-1 compound through maintaining endoplasmic reticulum (ER) and i-NOS homeostasis using immunoblot technique. Equal amount of protein (10 μg/well) from conditioned cell lysate (RT, DMSO, Fer-1 and Fer-1 + RT) was loaded in 12 % SDS-PAGE gel. After blotting the gel into the PVDF membrane it was treated using specific antibody to see its expression level. We only found the cleavage of native PARP-1 protein after 24 h RT treatment (Fig. 4a) as previously reported [16]. When SHSY-5Y cell were pre-treated with 1 μM of Fer-1 compound, 4 h prior to 500 nM RT exposure, we found no activation (cleavage; 89 kDa fragment) of PARP-1. We also found statistically significant decrease in the cleaved PARP-1 expression ($P = 0.0162$) when quantified using Image J software (Fig. 4b, white box indicative of cleaved PARP-1 over GAPDH). This data suggest that Fer-1 can inhibit the RT-induced PARP-1 cleavage in SHSY-5Y cells; a characteristic biochemical event of apoptosis.

3.5 Fer-1 Intervention in ER-mediated Stress Response

Rotenone increased significantly the 70 kilodalton heat shock protein (Hsp70) expression, as compared with the

A

Cytotoxicity Assay

Name	Concentration (μM)	Cell death (%)
Nitro analog (1)	12.5	20
	6.25	4
	3.13	0
Fer-1	12.5	3
	6.25	1
	3.13	0

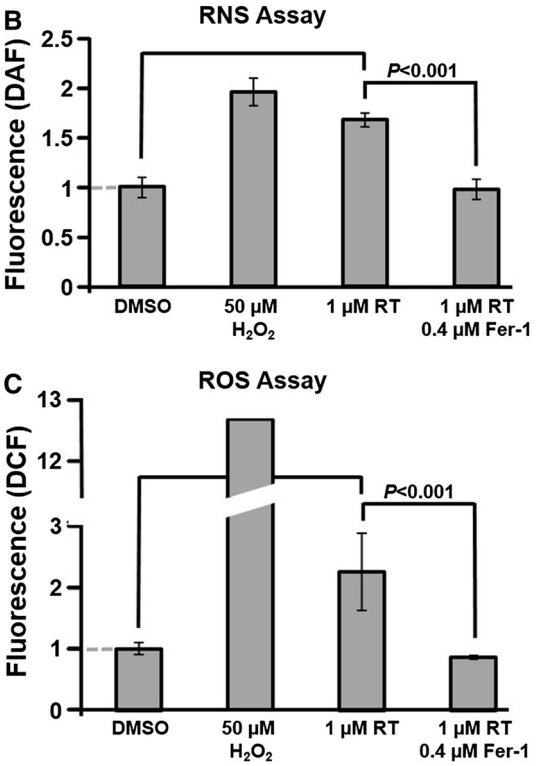

Fig. 3 Rotenone-induced RNS and ROS scavenged by Fer-1 pretreatment. **a** Cytotoxicity of **1**, **2** and rotoenone compounds. **b** and **c** Fer-1 treatment attenuates ROS and RNS levels induced by rotenone. The ROS/RNS levels were measured by DCFH-DA staining assay and analyzed at 24 h after Fer-1 treatment Statistical significance compared with untreated are illustrated as *P* value. Each *bar* represents the average of two replicates and the *error bars* their standard deviation. Negative control: DMSO treatment, positive control: 50 μM of Hydrogen peroxide (H_2O_2), Rotenone (1 μM) and Fer-1 (0.4 μM)

untreated cells ($P = 0.0008$; Fig. 4a; third row). Fer-1 compound pretreatment (4 h) before RT addition reduced the Hsp70 expression level drastically when compared with just RT treatment ($P = 0.0010$; Fig. 4b, the grey box is indicative of Hsp70). We used GAPDH (37 kDa) as a loading control. The X axis represents different treatment conditions, whereas Y axis denotes relative protein expression level over GAPDH expression. Hsp70 is over expressed under ER stress as a part of defensive mechanism [23]. Failure to cope up with the ER stress, often leads to activation of apoptotic pathway leading towards cell death [23]. Equal amount of protein (10 μg/well) from each treatment condition was loaded in 12 % SDS-PAGE. GAPDH (37 kDa) was used as a housekeeping loading control. Immunoblot data using anti-i-NOS antibody showed that RT clearly increased the expression of i-NOS (130 kDa). Interestingly, Fer-1 treatment alone for 24 h did not change the expression level of i-NOS in SHSY-5Y cell when compared with vehicle (0.02 % DMSO) treated cells. Nearly two fold increase in i-NOS level was quantified upon RT exposure alone in relation to vehicle treated condition ($P = 0.0141$; Fig. 4d). The significant finding is that 1 μM Fer-1 compound pretreatment (4 h prior to 500 nM RT exposure) inhibit the RT induced alteration of i-NOS expression in dopaminergic SHSY-5Y cell line (Fig. 4c, d; $P = 0.0048$). Quantification of HSP70 bands was normalized to the GAPDH bands by Image J software.

3.6 Fer-1 Mitigated Rotenone-induced α-syn Aggregation

Figure 5 shows the confocal fluorescence images of the effect of Fer-1 compound in α-syn aggregation in α-syn-SHSY-5Y cell. To check the efficacy of Fer-1 compound we decided to create stable α-syn-expressing neuronal SHSY-5Y cell line. SHSY-5Y cells were first transiently transfected with pCMV-6/α-syn plasmid and then selected using 900 μg/ml G418. Once got the stable cell line, different treatment conditions was employed to monitor the α-syn aggregation by using confocal microscope (Fig. 5a). The expression of α-syn in untreated SHSY-5Y cell was found homogeneously distributed in cytoplasm and perinuclear position. The long processes of SHSY-5Y cell also found to be rich with α-syn protein. Texas red-conjugated secondary antibody was used to stain the protein (red channel). Fer-1 treated cells and solvent control cells exhibited similar diffused α-syn expression and intensity pattern (Fig. 5a, b). The most significant change in α-syn intensity and pattern distribution was found after 500 nM RT treatment. First of all, the cells tend to clump together and α-syn found as cytoplasmic speckled mass, non-homogeneous inclusions (white arrow head) after 24 h RT exposure. Second, we found around two folds increased intensity of α-syn (red channel) upon RT treatment when compared with vehicle treated cells (Fig. 5b; $P = 0.0015$). In case of 1 μM Fer-1 compound pretreatment (4 h prior to RT exposure) resulted in dramatic decrease of specked shaped α-syn aggregates (white arrow head) when compared with RT exposure alone (Fig. 5b; $P = 0.0121$). The differential interference contrast (DIC) image (righteous panel of each image), merged with fluorescence channels, under 1 μM Fer-1 compound pretreatment condition showed increased vesicle formation (black arrow; may be

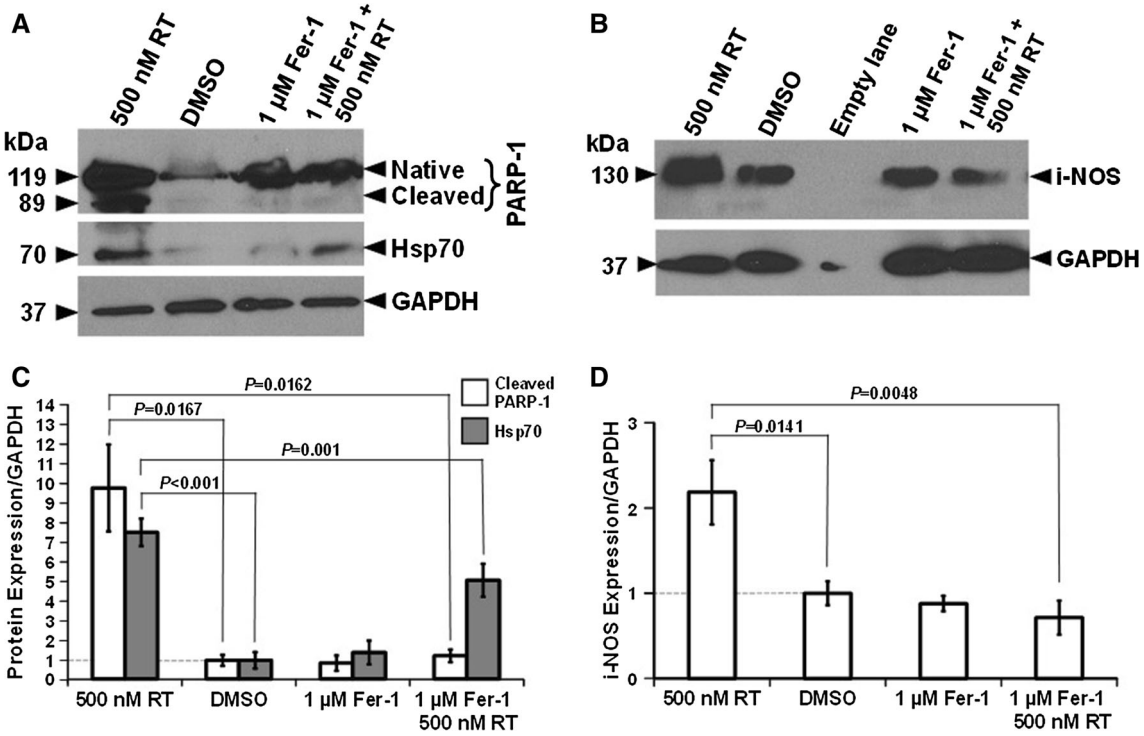

Fig. 4 Anti-apoptotic ability of Fer-1 through maintaining endoplasmic reticulum (ER) and i-NOS homeostasis. Immunoblot technique was used to detect the apoptotic activation: vehicle control (DMSO), Fer-1, rotenone and pretreatment with Fer-1 and then 24 h rotenone exposure. **a** Rotenone (RT) induced over expression of heat shock protein70 (Hsp70) is mitigated by 1 μM Fer-1 pretreatment. **b** Expression of ER-stress marker protein, Hsp70, is quantified under different treatment using Image J. **c** RT induced over expression of i-NOS is inhibited by 1 μM Fer-1 pretreatment. **d** Quantification of i-NOS expressions, after GAPDH normalization, using Image J. Statistical significance between samples is illustrated as *P* value (n = 3)

part of exocytosis) relative to all other treatment (Fig. 5a). Image J software was used to quantify the α-syn signal intensity, as depicted in Fig. 5b.

4 Discussion

We first synthesized the nitro analog (**1**) and Fer-1 compounds in the laboratory based on our recently reported work (Fig. 1b) [17–19]. We first sought to evaluate the morphology of SH-S5Y cells upon rotenone exposure alone and co-treated with Fer-1 (Fig. 2). The appearances of rotenone-induced morphological alterations in SH-S5Y cells, and the potential Fer-1 mitigating effect against rotenone insult, were study by using a series of bright field microscopic images captured in a live-cell mode. After rotenone treatment (for 24 h), cells started to detach, displaying an accentuated cell shape alteration, evidenced by spherical shape without protrusions indicative of cell detachment, and forming spherical cell aggregates (Fig. 2a; black arrows); this pattern was also observed in H_2O_2-treated cells, used as positive control for cytotoxicity (Fig. 2f; black arrows). These cellular morphological changes are suggestive of profound cytoskeletal disorganization, including loss of cellular anchoring proteins, characteristics of stress response to a toxic insult. In contrast, those rotenone-provoked morphological changes, indicative of stress response, were reverted when cells was incubated together with a mixture of both Fer-1 and rotenone (Fig. 2b). Hence, rotenone induces remarkable cell morphological changes and findings point out that Fer-1 possess prophylactic activity on rotenone-inflicted neurotoxic or neurodegenerative aggression on SH-S5Y cells. We then took advantage of the commercially available DPPH stable radical using a colorimetric assay [20] to assess the ability of the nitro compound (**1**) and Fer-1 to quench the stable radical [17, 18]. We reported that the nitro compound (**1**) did not inhibit the DPPH free radical, while Fer-1 showed 82 % inhibition compared to DMSO control [17, 18]. Finally we evaluated the cytotoxicity of the nitro-analog **1** and Fer-1 compounds against SH-SY5Y cells at three different concentrations (3.13, 6.25 and 12.5 μM). Our data showed that Fer-1 was not cytotoxic at concentrations up to 12.5 μM (Fig. 3b). Having morphological analysis of SH-S5Y cells exposed to rotenone, the antioxidant properties (DPPH data) and the cytotoxicity

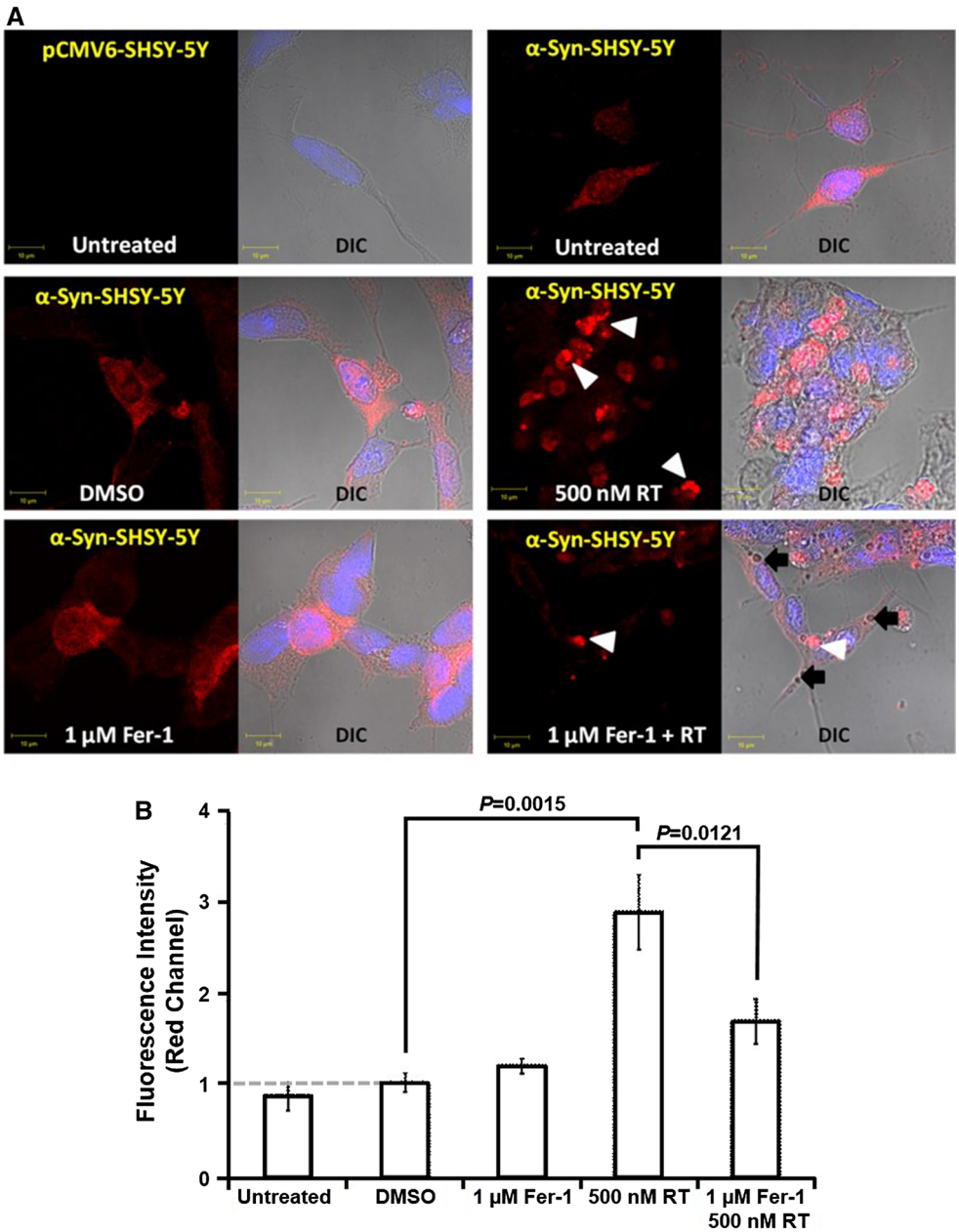

Fig. 5 Role of Fer-1 in α-syn aggregation in α-syn-SHSY-5Y cell. Cells transfected with pCMV6 empty vector, untreated α-syn-SHSY-5Y cells. Treated with DMSO 0.02 % v/v, treated with 1 μM Fer-1, cells exposed to rotenone (RT) (500 nM) for 24 h alone and cells treated with 1 μM Fer-1 for 4 h prior exposed to rotenone (500 nM) for 24 h are the different conditions used for this study (**a**, **b**). Confocal fluorescence images of SHSY-5Y cells after 100 % methanol fixation revealed the presence of α-syn cytoplasmic aggregates under different conditions (**a**). All the cells were counterstained with DAPI to stain the nucleus (*blue color*). *White arrow head* indicates aggregation of α-syn protein. *Black arrow* is representative of vesicle shown in DIC image. Quantification of α-syn (Texas Red; *red channel*) in SHSY-5Y cell line upon different treatment using Image J software from n = 200 cells indicated as mean ± SD (**b**). Statistical significance between pairs of samples is illustrated as *P* value. Each *scale bar* represents 10 μm. Each experiment was assessed in triplicate (Color figure online)

data (Fig. 3b) in our hand, we decided to quantify the ROS/RNS level under (i) rotenone treatment alone and (ii) rotenone co-treated with Fer-1 compound compared to DMSO treatment (Fig. 3c, d). To evaluate the neuroprotective effect of Fer-1 compound against rotenone-induced oxidative stress and based on the cytotoxicity data (Fig. 3b), we decided to use Fer-1 compound at 0.4 μM concentration which is unlikely to cause any cytotoxicity to the dopaminergic neuroblastoma SH-SY5Y cells, against rotenone at 1 μM that known to induce oxidative stress. We observed that Fer-1 compound inhibited the ROS/RNS generated under rotenone insult in SH-SY5Y cells. Altogether, these findings reveals the ability of Fer-1 to reduce both RNS and ROS intracellular levels provoked by RT, ultimately demonstrating that Fer-1 can become a promising treatment for RNS and ROS-induced PD. A recent study showed that 500 nM of rotenone can induce apoptotic cell death upon excessive generation of radical species especially RNS [16]. We therefore investigated if Fer-1 compound could mitigate the toxic effect of rotenone (Fig. 4). We looked at the cleavage of Poly (ADP-ribose) polymerase-1 (PARP-1), a marker protein for apoptotic activation, by immuno-blotting technique (Fig. 4a, b). To validate our hypothesis of the protective effect of Fer-1 of PARP-1 cleavage under RT treatment, we used the same concentration of rotenone (500 nM), as was reported

previously [16] to mimic the apoptotic cell death, against 1 μM of Fer-1. Our data suggest that Fer-1 is likely capable of protecting the cells from controlled death by reducing the ER stress level. On the other hand, lipopolysaccharide (LPS), known as a i-NOS inducer, mediated PD model suggest the involvement of aggregated α-syn in glia cell activation and release of excessive RNS [24]. Previous studies showed that RT-induced RNS increase is due to the overexpression of iNOS [25, 26]. In addition, RNS reported to potentially hinder protein folding, lipid oxidation and other biomolecules [16]. In this study we decided to look at the i-NOS expression level upon RT as well as Fer-1 treatment (Fig. 4c, d). This study suggest that RT exposure induce excessive RNS production by over expressing i-NOS which in turn activates the catalytic carboxy-terminal domain (89 kDa) by cleaving off amino-terminal DNA binding domain (24 kDa) of PARP-1 leading towards apoptosis. In contrary, the Fer-1 compound suppressed RT induced activation of apoptotic pathway by regulating i-NOS expression (Fig. 4c, d). In PD histopathology α-syn is the major constituent of Lewy body [5]. The cause and effect relationship between reactive species and α-syn aggregate formation is still unknown. We finally assessed if Fer-1 could mitigated rotenone-induced α-syn aggregation in our created stable α-syn-expressing neuronal SHSY-5Y cell line (Fig. 5). The α-syn cytoplasmic distribution was investigated after α-syn gene transfection of human dopaminergic neuroblastoma SH-SY5Y cells line and visualized with antibodies labeling technique in conjunction with confocal microscopic images. As depicted in Fig. 5, two distinct distribution patterns of α-syn (red channel) were distinguished: ample or restricted subcellular cytoplasmic localization. In untreated control cells, red fluorescence signal (α-syn) was localized in a more ample distribution non-punctuated pattern, observed in the whole cytoplasm of the cells (Fig. 5); whereas in rotenone-treated cells, red signal was predominantly confined within discrete intracytoplasmic punctuated regions, interpreted as α-syn aggregation (Fig. 5). Also, our data exhibited predominantly diffused non-punctuated α-syn localization in the cytosol of cells treated with Fer-1 and with rotenone concomitantly (Fig. 5). Therefore, our result showed clearly the efficacy of Fer-1 compound in reducing RT-induced α-syn aggregation in SHSY-5Y cell (Fig. 5).

In conclusion, we have investigated the neuroprotective effect of Fer-1 compound, as a novel scaffold, against rotenone induced cell death by using SHSY-5Y dopaminergic neuroblastoma cells. This study revealed that Fer-1 attenuate the apoptotic stimuli evidenced by reducing rotenone-induced PARP1 cleavage; a biochemical hallmark of apoptosis. We also provided cellular and non-cellular evidence that Fer-1 is acting as a radical scavenger which will prevent the formation the S-nitrosyl-PDI complex. Indeed, our data showed the ability of Fer-1 in protecting (i) the cell from rotenone-induced apoptosis, (ii) Hsp70 expression, which is an indicator of ER stress, and (iii) i-NOS expression and (iv) the possible aggregation of α-syn in stable SHSY-5Y cell line (Figs. 4, 5). These results suggest that Fer-1 mitigates nitrosative stress-induced synphilin-1 aggregates in SH-SY5Y cell lines. Currently, we are investigating the creation of Fer-1 analogs with high potency, solubility, stability and better blood–brain barrier permeation for further evaluation in in vivo models.

Acknowledgments Authors thank the staff of the Cytometry, Screening and Imaging Core Facility, supported by grant 2G12MD007592 from National Institute on Minority Health and Health Disparities (NIMHD), a component of the National Institutes of Health (NIH). Also, authors thank the Border Biomedical Research Center-UTEP for a pilot grant (NIMHD/G12MD007592) to R.S. and the University of Texas URI for a grant to R.S. This study was supported in part by the STAR award to KF and the Alzheimer's disease Research Foundation to MN. CV is funded by an undergraduate fellowship from the Research Initiative for Scientific Enhancement (RISE) program (NIH/NIGMS grant # R25GM069621-11) at UTEP.

References

1. Ferraro G, Sardo P (2004) Nitric oxide and brain hyperexcitability. In Vivo 18:357–366
2. Choudhari SK, Chaudhary M, Bagde S, Gadbail AR, Joshi V (2013) Nitric oxide and cancer: a review. World J Surg Oncol 11:118
3. Mattson MP (2000) Apoptosis in neurodegenerative disorders. Nat Rev Mol Cell Biol 2:120–129
4. Radi E, Formichi P, Battisti C, Federico A (2014) Apoptosis and oxidative stress in neurodegenerative diseases. J Alzheimers Dis 42(Suppl 3):S125–S152
5. Su B, Liu H, Wang X, Chen SG, Siedlak SL, Kondo E, Choi R, Takeda A, Castellani RJ, Perry G, Smith MA, Zhu X, Lee HG (2009) Ectopic localization of FOXO3a protein in Lewy bodies in Lewy body dementia and Parkinson's disease. Mol Neurodegener 4:32
6. Gispert-Sanchez S, Auburger G (2006) The role of protein aggregates in neuronal pathology: guilty, innocent, or just trying to help? J Neural Transm Suppl 70:111–117
7. Satoh MS, Lindahl T (1992) Role of poly(ADP-ribose) formation in DNA repair. Nature 356:356–358
8. Tan S, Sagara Y, Liu Y, Maher P, Schubert D (1998) The regulation of reactive oxygen species production during programmed cell death. J Cell Biol 141:1423–1432
9. Grek C, Townsend DM (2014) Protein disulfide isomerase superfamily in disease and the regulation of apoptosis. Endoplasmic Reticulum Stress Dis 1:4–17
10. Townsend DM, Manevich Y, He L, Xiong Y, Bowers RR Jr, Hutchens S, Tew KD (2009) Nitrosative stress-induced s-glutathionylation of protein disulfide isomerase leads to activation of the unfolded protein response. Cancer Res 69:7626–7634
11. Uehara T, Nakamura T, Yao D, Shi ZQ, Gu Z, Ma Y, Masliah E, Nomura Y, Lipton SA (2006) S-nitrosylated protein-disulphide isomerase links protein misfolding to neurodegeneration. Nature 441:513–517

12. Mattson MP (2006) Nitro-PDI incites toxic waste accumulation. Nat Neurosci 9:865–867
13. Uehara T (2007) Accumulation of misfolded protein through nitrosative stress linked to neurodegenerative disorders. Antioxid Redox Signal 9:597–601
14. Pal R, Cristan EA, Schnittker K, Narayan M (2010) Rescue of ER oxidoreductase function through polyphenolic phytochemical intervention: implications for subcellular traffic and neurodegenerative disorders. Biochem Biophys Res Commun 392: 567–571
15. Pal R, Miranda M, Narayan M (2011) Nitrosative stress-induced Parkinsonian Lewy-like aggregates prevented through polyphenolic phytochemical analog intervention Biochem. Biophys Res Commun 404:324–329
16. Kabiraj P, Marin J, Varela-Ramirez A, Zubia E, Narayan M (2014) Ellagic acid mitigates SNO-PDI induced aggregation of Parkinsonian biomarkers. ACS Chem Neurosci 5:1209–1920
17. Dixon SJ, Lemberg KM, Lamprecht MR, Skouta R, Zaitsev EM, Gleason CE, Patel DN, Bauer AJ, Cantley AM, Yang WS, Morrison B, Stockwell BR (2012) Ferroptosis: an iron-dependent form of nonapoptotic cell death. Cell 149:1060–1072
18. Skouta R, Dixon SJ, Wang J, Dunn DE, Orman M, Shimada K, Rosenberg PA, Lo DC, Weinberg JM, Linkermann A, Stockwell BR (2014) Ferrostatins inhibit oxidative lipid damage and cell death in diverse disease models. J Am Chem Soc 136:4551–4556
19. Linkermann A, Skouta R, Himmerkus N, Mulay SR, Dewitz C, De Zen F, Prokai A, Zuchtriegel G, Krombach F, Welz PS, Weinlich R, Vanden Berghe T, Vandenabeele P, Pasparakis M, Bleich M, Weinberg JM, Reichel CA, Bräsen JH, Kunzendorf U, Anders HJ, Stockwell BR, Green DR, Krautwald S (2014) Synchronized renal tubular cell death involves ferroptosis. PNAS 111:16836–16841
20. Blois MS (1958) Antioxidant determinations by the use of a stable free radical. Nature 181:1199–1200
21. Robles-Escajeda E, Lerma D, Nyakeriga AM, Ross JA, Kirken RA, Aguilera RJ, Varela-Ramirez A (2013) Searching in mother nature for anti-cancer activity: anti-proliferative and pro-apoptotic effect elicited by green barley on leukemia/lymphoma cells. PLoS ONE 8(9):e73508
22. Gant VU Jr, Moreno S, Varela-Ramirez A, Johnson KL (2014) Two membrane-associated regions within the Nodamura virus RNA-dependent RNA polymerase are critical for both mitochondrial localization and RNA replication. J Virol 88(11): 5912–5926
23. Cabral Miranda F, Adão-Novaes J, Hauswirth WW, Linden R, Petrs-Silva H, Chiarini LB (2015) CHIP, a carboxy terminus HSP-70 interacting protein, prevents cell death induced by endoplasmic reticulum stress in the central nervous system. Front Cell Neurosci 8:438
24. Thomas MP, Chartrand K, Reynolds A, Vitvitsky V, Banerjee R, Gendelman HE (2007) Ion channel blockade attenuates aggregated alpha synuclein induction of microglial reactive oxygen species: relevance for the pathogenesis of Parkinson's disease. J Neurochem 100:503–519
25. Drechsel DA, Patel M (2008) Role of reactive oxygen species in the neurotoxicity of environmental agents implicated in Parkinson's disease. Free Radic Biol Med 44:1873
26. Dias V, Junn E, Mouradian MM (2013) The role of oxidative stress in Parkinson's disease. J Parkinson's Dis 3:461